

Spontaneous strain glass to martensite transition in ferromagnetic Ni-Co-Mn-Ga strain glass

Yu Wang, Chonghui Huang, Haijun Wu, Jinghui Gao, Sen Yang, Dong Wang, Xiangdong Ding, Xiaoping Song, and Xiaobing Ren

Citation: *Applied Physics Letters* **102**, 141909 (2013); doi: 10.1063/1.4799151

View online: <http://dx.doi.org/10.1063/1.4799151>

View Table of Contents: <http://scitation.aip.org/content/aip/journal/apl/102/14?ver=pdfcov>

Published by the AIP Publishing

Advertisement:



Goodfellow

metals • ceramics • polymers
composites • compounds • glasses

Save 5% • Buy online

70,000 products • Fast shipping

www.goodfellowusa.com

Spontaneous strain glass to martensite transition in ferromagnetic Ni-Co-Mn-Ga strain glass

Yu Wang,^{1,a)} Chonghui Huang,¹ Haijun Wu,² Jinghui Gao,² Sen Yang,¹ Dong Wang,^{1,2} Xiangdong Ding,¹ Xiaoping Song,^{1,b)} and Xiaobing Ren^{1,2,3}

¹MOE Key Laboratory for Nonequilibrium Synthesis and Modulation of Condensed Matter and State Key Laboratory for Mechanical Behavior of Materials, Xi'an Jiaotong University, Xi'an 710049, China

²Multi-disciplinary Materials Research Center, Frontier Institute of Science and Technology, Xi'an Jiaotong University, Xi'an 710049, China

³National Institute for Materials Science, 1-2-1 Sengen, Tsukuba 305-0047, Ibaraki, Japan

(Received 16 December 2012; accepted 19 March 2013; published online 11 April 2013)

We report that a spontaneous strain glass to martensite (STG-M) transition occurs in a $\text{Ni}_{45}\text{Co}_{10}\text{Mn}_{20}\text{Ga}_{25}$ ferromagnetic strain glass. The signatures of the spontaneous STG-M transition of $\text{Ni}_{45}\text{Co}_{10}\text{Mn}_{20}\text{Ga}_{25}$ ferromagnetic strain glass are stronger than those of $\text{Ti}_{50}\text{Ni}_{44.5}\text{Fe}_{5.5}$ strain glass reported previously. Such a difference is attributed to that the martensitic terminal of the former has larger elastic anisotropy than that of the later. The spontaneous STG-M transition in this ferromagnetic strain glass is due to that the delicate competition between the kinetic limitation and the martensitic thermodynamic driving force changes with temperature. © 2013 American Institute of Physics. [<http://dx.doi.org/10.1063/1.4799151>]

Martensitic/ferroelastic transition undergoes diffusion-less structure change from a high temperature open structure to a low temperature close packed structure, during which long range lattice strain ordering is established in martensite.¹ When point defects are introduced into martensitic system, kinetic hindrance for its martensitic transition is produced.² When defect content increases to above a crossover composition, the kinetic limitation can be even stronger than the thermodynamic driving force of martensite. Thus, the spontaneous martensitic transition becomes kinetically forbidden and is suppressed completely.² However, the system undergoes a strain glass transition instead and transforms into a meta-stable strain glass state, in which nano-sized martensitic domains (short range ordered strains) are frozen in random fashion.^{3,4} Previous studies proposed that martensitic nano-domain structure can be formed by local fluctuation of martensitic transition temperature associated with local composition variation⁵⁻⁷ or be produced by the local stress field of point defects.⁸⁻¹⁰ It was further shown that the strain glass alloy located in the crossover composition regime undergoes a strain glass transition at high temperature and then a spontaneous strain glass to martensite (STG-M) transition at low temperature, during which the nano-sized martensitic domains transforms spontaneously into macro-sized martensite.¹¹ These findings demonstrate that the thermodynamic and kinetic factors may play delicate competition in strain glass system,^{4,11} which dominates its transition behaviors.

Strain glass has been found in diverse defect doped martensitic systems^{3,11,12} and was reported to exhibit functional properties including shape memory effect, superelasticity, and stress-controlled damping behavior^{13,14} which makes it a subject with practical importance and fundamental interest. Recently, a ferromagnetic strain glass with coexisting short

range strain order and long range magnetic order was reported in Co doped ferromagnetic martensitic Ni-Mn-Ga system.¹⁵ This finding extends the research horizon of strain glass and may lead to the finding of more functional properties.

The spontaneous STG-M transition was initially reported in the non-magnetic $\text{Ti}_{50}\text{Ni}_{44.5}\text{Fe}_{5.5}$ strain glass.¹¹ Whether such a transition can occur in ferromagnetic strain glass or not is unknown so far. Moreover, it is known that the martensitic transition is associated with well-defined soft crystallographic directions of parent phase.^{16,17} Thus, the transforming behaviors of defect doped martensitic systems are closely related to the elastic anisotropy of their martensitic terminal.^{5,18} The $\text{Ti}_{50}\text{Ni}_{44.5}\text{Fe}_{5.5}$ strain glass with spontaneous STG-M transition is formed by doping defects into the Ti-Ni martensitic terminal with low elastic anisotropy.^{1,18} Few investigations of spontaneous STG-M transition were performed in the strain glass system derived from the high elastically anisotropic martensitic terminal. Thus, the universality of the spontaneous STG-M transition of strain glass system is far from proved.

In this letter, we will show the evidences for the spontaneous STG-M transition in a ferromagnetic strain glass $\text{Ni}_{45}\text{Co}_{10}\text{Mn}_{20}\text{Ga}_{25}$ located in the crossover composition regime. The $\text{Ni}_{45}\text{Co}_{10}\text{Mn}_{20}\text{Ga}_{25}$ ferromagnetic strain glass is formed by doping Co into Ni-Mn-Ga ferromagnetic martensitic system, of which elastic anisotropy is high.^{19,20} Our results reveal that the spontaneous STG-M transition in this ferromagnetic strain glass exhibits stronger transforming signatures than those observed in $\text{Ti}_{50}\text{Ni}_{44.5}\text{Fe}_{5.5}$ strain glass, of which the corresponding martensitic terminal possesses low elastic anisotropy. The magnetic property of the sample changes during its spontaneous STG-M transition. Moreover, its spontaneous transition temperature can be changed by applying magnetic field, obeying the thermodynamic rule. The formation of this spontaneous STG-M transition is also discussed through the competition between the thermodynamic and kinetic factors in the system.

^{a)}Email: yuwang@mail.xjtu.edu.cn

^{b)}Email: songxp@mail.xjtu.edu.cn

The $\text{Ni}_{45}\text{Co}_{10}\text{Mn}_{20}\text{Ga}_{25}$ alloy was fabricated by arc melting 99.9% pure metals of Ni, Co, Mn, and Ga in argon atmosphere. The as-cast sample was annealed at 1173 K for 24 h in evacuated quartz tubes and subsequently quenched into room temperature water. The dynamic mechanical analysis (DMA) was performed with 3-point bending clamp to characterize the transitions of the sample. The temperature dependence of magnetization was also measured by vibrating sample magnetometer (VSM) to identify the magnetic transition. The transforming latent heat was measured by a differential scanning calorimeter (DSC). Moreover, *in-situ* X-ray diffraction (XRD) measurement and transmission electron microscopy (TEM) observation were performed to monitor the temperature evolution of the average structure and domain configuration of the sample.

Fig. 1(a) shows the dynamic mechanical properties of solution treated $\text{Ni}_{45}\text{Co}_{10}\text{Mn}_{20}\text{Ga}_{25}$ alloy, which displays broad storage modulus dips and internal friction peaks with frequency dispersion at $T > T^*$. The corresponding DSC measurement (Fig. 1(b)) does not show any peak at this temperature range, demonstrating no structure transition at $T > T^*$. These experimental results reveal typical characteristics of strain glass^{3,4} and demonstrate that the sample undergoes strain glass transition at high temperature. Moreover, the temperature dependence of magnetization in Fig. 1(c) shows that the freezing temperature T_g of the $\text{Ni}_{45}\text{Co}_{10}\text{Mn}_{20}\text{Ga}_{25}$ strain glass is well below the Curie temperature (T_C) of its

ferromagnetic transition (inset of Fig. 1(c)). This demonstrates that its strain glass state is ferromagnetic.

By comparison, the transition behaviors of $\text{Ni}_{45}\text{Co}_{10}\text{Mn}_{20}\text{Ga}_{25}$ ferromagnetic strain glass show quite different characteristics at $T < T^*$. As depicted in Fig. 1(a), its storage modulus exhibits a softening upon cooling below T^* and then a sharp decrease at a lower temperature T_S . This steep drop in storage modulus resembles that of the onset of martensitic transition.^{21,22} Due to the lowest temperature limitation of our dynamic mechanical analyzer, the complete sharp modulus dips and internal friction peaks cannot be measured despite they are expected to appear on further cooling. However, the DSC curve (Fig. 1(b)) shows an obvious latent heat peak below T_S , revealing the appearance of martensitic transition. Moreover, the temperature dependence of magnetization (Fig. 1(c)) also shows a drop at T_S , which is similar to the behavior of the martensitic transition in Ni-Mn-Ga based ferromagnetic shape memory alloy.²³ Thus, all the above experimental results demonstrate the existence of a low temperature spontaneous STG-M transition following the high temperature strain glass transition in the system. The T_S (138 K) is the transition temperature of its spontaneous STG-M transition.

The temperature evolution of the average structure of $\text{Ni}_{45}\text{Co}_{10}\text{Mn}_{20}\text{Ga}_{25}$ ferromagnetic strain glass is characterized by *in-situ* XRD measurement. As shown in Fig. 2(a), the XRD pattern of the sample can be indexed as the $L2_1$ cubic structure from 303 K (well above T_g) to 143 K (well below T_g and slightly above T_S). This is consistent with the fact that the average structure keeps invariant during strain glass transition. However, at the temperature of 93 K below T_S , the XRD pattern of the sample changes apparently and can be indexed as a tetragonal martensitic structure. Thus, the spontaneous transition from strain glass into martensite was further confirmed by average structure determination.

In-situ TEM observation was also performed to characterize the microstructure evolution during the strain glass transition and spontaneous STG-M transition of the sample. At 300 K, the $\text{Ni}_{45}\text{Co}_{10}\text{Mn}_{20}\text{Ga}_{25}$ ferromagnetic strain glass exhibits nano-domain morphology (Fig. 2(b)) above T_g . The size of these martensitic nano-domains is within 10 nm–30 nm, which is similar to those observed in $\text{Ni}_{43}\text{Co}_{12}\text{Mn}_{20}\text{Ga}_{25}$ ferromagnetic strain glass.¹⁵ The martensitic nano-domains grow slightly when cooling from 300 K to 190 K. Their size remains below 50 nm essentially from above T_g to T^* (below T_g), as shown in Figs. 2(b)–2(d). It should be mentioned that the precursor state of some other ferromagnetic martensitic systems also exhibits similar nano-domain structure above the martensitic transition temperature, such as the precursory tweed texture of Co-Ni-Al ferromagnetic martensitic alloy.²⁴ However, being different from the strain glass of Ni-Co-Mn-Ga system, the precursor state of Co-Ni-Al system does not exhibit dynamic mechanical anomaly. This demonstrates that the precursory tweed nano-domains of Co-Ni-Al martensitic system do not accompany transition processes, while the martensitic nano-domains of Ni-Co-Mn-Ga strain glass system undergo a freezing transition.

The martensitic nano-domains of $\text{Ni}_{45}\text{Co}_{10}\text{Mn}_{20}\text{Ga}_{25}$ ferromagnetic strain glass grow continuously and become even bigger (Fig. 2(e)) upon further cooling to 140 K ($\sim T_S$). Moreover, a few plate like domains with the size of around

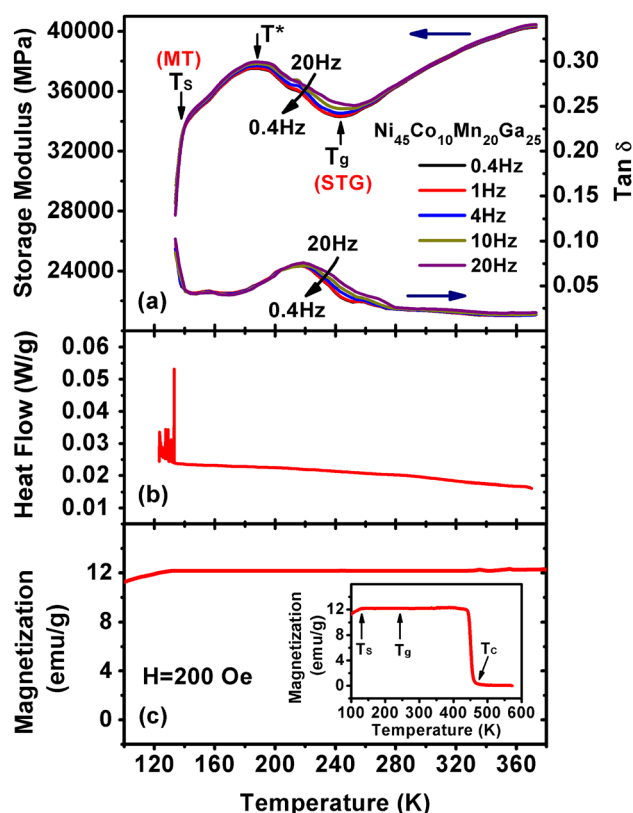


FIG. 1. The transforming behaviors of $\text{Ni}_{45}\text{Co}_{10}\text{Mn}_{20}\text{Ga}_{25}$ ferromagnetic strain glass during its strain glass transition and spontaneous STG-M transition. (a) The dynamic mechanical properties, (b) DSC curve, and (c) temperature dependence of magnetization of the sample. The inset of (c) shows that the Curie temperature (T_C) of its ferromagnetic transition is well above its strain glass transition temperature (T_g) and spontaneous STG-M transition temperature (T_S).

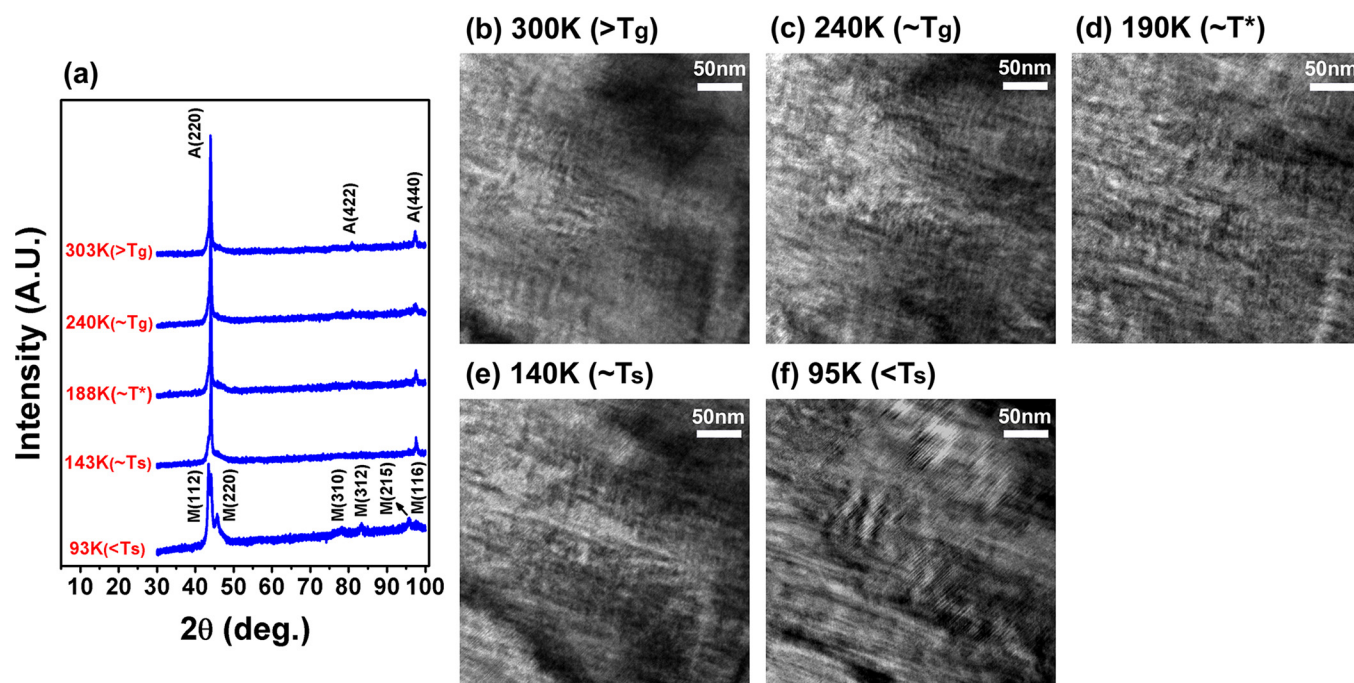


FIG. 2. (a) Average structure evolution of $\text{Ni}_{45}\text{Co}_{10}\text{Mn}_{20}\text{Ga}_{25}$ ferromagnetic strain glass from 303 K to 93 K, which spans the temperature regime of its strain glass transition and spontaneous STG-M transition. (b)-(f) shows the microscopic domain structure of the sample at 300 K, 240 K, 190 K, 140 K, and 95 K, respectively.

100 nm can be recognized at this temperature, which demonstrates that martensite plates start to grow up near the spontaneous STG-M transition temperature T_S . When the temperature reaches 93 K below T_S , the martensite plates grow not only in size (150 nm–200 nm) but also in density (Fig. 2(f)). The sample is essentially occupied by the martensitic plates and the martensitic twin morphology with straight twin boundary can be readily observed. Similar martensitic twin morphology was also observed in $\text{Ni}_{50}\text{Mn}_{20}\text{Ga}_{25}$ ferromagnetic martensitic alloy when we did TEM observation.

The spontaneous STG-M transition of $\text{Ni}_{45}\text{Co}_{10}\text{Mn}_{20}\text{Ga}_{25}$ ferromagnetic strain glass exhibits different features from those observed in $\text{Ti}_{50}\text{Ni}_{44.5}\text{Fe}_{5.5}$ strain glass. The $\text{Ni}_{45}\text{Co}_{10}\text{Mn}_{20}\text{Ga}_{25}$ strain glass exhibits strong anomaly in its storage modulus and internal friction and obvious latent heat peak during its spontaneous STG-M transition (Figs. 1(a) and 1(b)). However, the $\text{Ti}_{50}\text{Ni}_{44.5}\text{Fe}_{5.5}$ strain glass displays a small kink in its storage modulus, a small hump in its internal friction and no obvious latent heat peak was reported during its spontaneous STG-M transition.¹¹ Moreover, the martensite plates (Fig. 2(f)) in $\text{Ni}_{45}\text{Co}_{10}\text{Mn}_{20}\text{Ga}_{25}$ strain glass have the size of 150 nm–200 nm below T_S , which are larger than those (~100 nm) of $\text{Ti}_{50}\text{Ni}_{44.5}\text{Fe}_{5.5}$ strain glass.¹¹ Such differences of the spontaneous STG-M transitions for these two strain glass systems are because they are formed by doping defects into the martensitic terminals with different elastic anisotropy. Recent theoretical simulation results show that the martensitic material with high elastic anisotropy possesses high ability to resist disorder (or defects) and strong tendency to transform into martensite.^{5,6} The elastic anisotropy is about 16–23 above the martensitic transition temperature (T_M) of Ni-Mn-Ga martensitic alloy,^{19,20} while it remains within 2–3 above the T_M of Ti-Ni based martensitic alloy.¹ Since the martensitic terminal of the $\text{Ni}_{45}\text{Co}_{10}\text{Mn}_{20}\text{Ga}_{25}$ strain glass has higher elastic

anisotropy than that of the $\text{Ti}_{50}\text{Ni}_{44.5}\text{Fe}_{5.5}$ strain glass, the spontaneous STG-M transition of the former shows stronger transforming ability and signatures than that of the later.

Fig. 3 shows the magnetization vs. temperature curves measured under different magnetic fields for $\text{Ni}_{45}\text{Co}_{10}\text{Mn}_{20}\text{Ga}_{25}$ ferromagnetic strain glass. The curve measured at 0.8 T reveals that the saturation magnetization drops upon cooling below its spontaneous STG-M transition temperature T_S . Moreover, the T_S decreases with increasing magnetic field, which shows a linear dependence (inset of

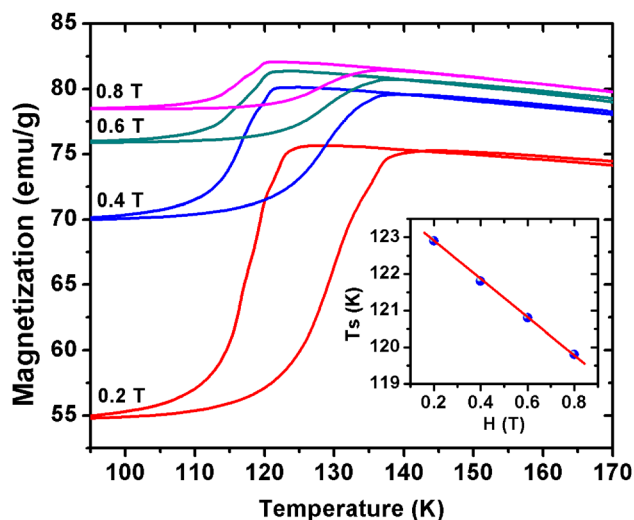


FIG. 3. The magnetization vs. temperature curves measured under different magnetic fields for $\text{Ni}_{45}\text{Co}_{10}\text{Mn}_{20}\text{Ga}_{25}$ ferromagnetic strain glass. The inset shows that its spontaneous STG-M transition temperature T_S decreases linearly with increasing magnetic field, obeying Clausius-Clapeyron relationship.

Fig. 3) conforming to the Clausius-Clapeyron relationship of first-order phase transitions:²⁵

$$\frac{dT}{dH} = -\frac{\Delta M}{\Delta S},$$

where ΔM and ΔS are the magnetization change and the entropy change during the transition, respectively. This demonstrates the spontaneous STG-M transition in this ferromagnetic strain glass obeys thermodynamic rule and is essentially dominated by thermodynamics.

The strain glass transition and spontaneous STG-M transition in $\text{Ni}_{45}\text{Co}_{10}\text{Mn}_{20}\text{Ga}_{25}$ ferromagnetic strain glass are due to the competition between the thermodynamic driving force of martensite and kinetic limitation in the system. These two factors play a dominate role alternately upon cooling, leading to the anomalies in its storage modulus. At the temperature above T_g , the kinetic limitation is trial and the martensitic state is energetically unstable.^{4,11} The sample stays in its ergodic unfrozen state with dynamically disordered strains. The unfrozen state shows heterophase fluctuation (flipping of instantaneous martensitic nano-domains) and its fluctuation amplitude increases upon decreasing temperature.²⁶ This leads to the lattice softening (decrease of storage modulus) on cooling at $T > T_g$ (Fig. 1(a)). When temperature decreases to below T_g , kinetic limitation becomes significant before martensite become energetically stable, resulting in the strain glass transition.^{4,11} Thus, the flipping of instantaneous nano-domains slows down, which leads to the lattice hardening (increase of storage modulus) on cooling below T_g (Fig. 1(a)).

On further cooling to below T^* , the martensitic state starts to become energetically stable. Nevertheless, the martensitic driving force is not large enough to overcome the kinetic limitation slightly below T^* . The sample cannot transform into martensite but stays in the meta-stable strain glass state. However, due to the existence of martensitic driving force, the already “frozen” nano-domains can grow gradually on cooling. This causes the lattice softening on cooling below T^* (Fig. 1(a)). When temperature decreases to T_S well below T^* , the martensitic driving force becomes large enough to overcome the kinetic limitation, which drives the system to transform from frozen strain glass to martensite, i.e., the spontaneous STG-M transition occurs. The nano-domains grow rapidly during the spontaneous STG-M transition to form macro-scale martensite plates. This accounts for the steep drop in its storage modulus at T_S (Fig. 1(a)).

The kinetic limitation of strain glass system originates from the flipping energy barriers of martensitic nano-domains, which can be created by disorder such as random distribution of local transition temperatures and random local stresses.^{6,8} From our experimental results, it can be summarized that the kinetic limitation is not the only factor to control the switching of martensitic nano-domains. The switching ability of the nano-domains for strain glass systems can be promoted by strong martensitic driving force and high elastic anisotropy of their martensitic terminals.^{6,27}

In conclusion, we found the existence of a spontaneous STG-M transition in a $\text{Ni}_{45}\text{Co}_{10}\text{Mn}_{20}\text{Ga}_{25}$ ferromagnetic

strain glass. The signatures of the spontaneous STG-M transition of $\text{Ni}_{45}\text{Co}_{10}\text{Mn}_{20}\text{Ga}_{25}$ ferromagnetic strain glass are stronger than those of $\text{Ti}_{50}\text{Ni}_{44.5}\text{Fe}_{5.5}$ strain glass. This is because the martensitic terminal of the former has larger elastic anisotropy than that of the later. The strain glass transition and its followed spontaneous STG-M transition in this ferromagnetic strain glass are attributed to the competition between the kinetic limitation and the martensitic thermodynamic driving force. These two factors play a dominate role alternately upon temperature change, leading to these two transitions. This finding demonstrates that the spontaneous STG-M transition is a general phenomenon in strain glass systems.

The present work was financially supported by National Natural Science Foundation of China (Grant Nos. 51101118, 51071117, and 51207121), National Basic Research Program of China (Grant Nos. 2012CB619401 and 2010CB631003), and Program for New Century Excellent Talents in University and the Fundamental Research Funds for Central Universities of China.

¹K. Otsuka and X. Ren, *Prog. Mater. Sci.* **50**, 511 (2005).

²R. Vasseur and T. Lookman, *Phys. Rev. B* **81**, 094107 (2010).

³S. Sarkar, X. Ren, and K. Otsuka, *Phys. Rev. Lett.* **95**, 205702 (2005).

⁴Y. Wang, X. Ren, K. Otsuka, and A. Saxena, *Acta Mater.* **56**, 2885 (2008).

⁵P. Lloveras, T. Castán, M. Porta, A. Planes, and A. Saxena, *Phys. Rev. Lett.* **100**, 165707 (2008).

⁶P. Lloveras, T. Castán, M. Porta, A. Planes, and A. Saxena, *Phys. Rev. B* **80**, 054107 (2009).

⁷S. Kartha, J. A. Krumhansl, J. P. Sethna, and L. K. Wickham, *Phys. Rev. B* **52**, 803 (1995).

⁸D. Wang, Y. Z. Wang, Z. Zhang, and X. Ren, *Phys. Rev. Lett.* **105**, 205702 (2010).

⁹S. Semenovskaya and A. G. Khachatryan, *Acta Mater.* **45**, 4367 (1997).

¹⁰Y. Wang and A. G. Khachatryan, *Acta Mater.* **45**, 759 (1997).

¹¹J. Zhang, Y. Wang, X. Ding, Z. Zhang, Y. Zhou, X. Ren, D. Wang, Y. Ji, M. Song, K. Otsuka, and J. Sun, *Phys. Rev. B* **84**, 214201 (2011).

¹²Y. Zhou, D. Xue, X. Ding, K. Otsuka, J. Sun, and X. Ren, *Appl. Phys. Lett.* **95**, 151906 (2009).

¹³Y. Wang, X. Ren, and K. Otsuka, *Phys. Rev. Lett.* **97**, 225703 (2006).

¹⁴Y. Wang, X. Song, X. Ding, S. Yang, J. Zhang, X. Ren, and K. Otsuka, *Appl. Phys. Lett.* **99**, 051905 (2011).

¹⁵Y. Wang, C. Huang, J. Gao, S. Yang, X. Ding, X. Song, and X. Ren, *Appl. Phys. Lett.* **101**, 101913 (2012).

¹⁶S. M. Shapiro, B. X. Yang, Y. Noda, L. E. Tanner, and D. Schryvers, *Phys. Rev. B* **44**, 9301 (1991).

¹⁷A. Zheludev, S. M. Shapiro, P. Wochner, and L. E. Tanner, *Phys. Rev. B* **54**, 15045 (1996).

¹⁸Y. Murakami, H. Shibuya, and D. Shindo, *J. Microsc.* **203**, 22 (2001).

¹⁹L. Dai, J. Cullen, J. Cui, and M. Wuttig, *Mater. Res. Soc. Symp. Proc.* **785**, D2.2.1 (2004).

²⁰J. Worgull, E. Petit, and J. Trevisono, *Phys. Rev. B* **54**, 15695 (1996).

²¹V. A. Chernenko, C. Seguí, E. Cesari, J. Pons, and V. V. Kokorin, *Phys. Rev. B* **57**, 2659 (1998).

²²C. Seguí, E. Cesari, J. Pons, and V. Chernenko, *Mater. Sci. Eng., A* **370**, 481 (2004).

²³V. V. Khovailo, K. Oikawa, C. Wedel, T. Takagi, T. Abe, and K. Sugiyama, *J. Phys.: Condens. Matter* **16**, 1951 (2004).

²⁴Y. Murakami, D. Shindo, K. Oikawa, R. Kainuma, and K. Ishida, *Acta Mater.* **50**, 2173 (2002).

²⁵L. Mañosa, X. Moya, A. Planes, T. Krenke, M. Acet, and E. F. Wassermann, *Mater. Sci. Eng., A* **481–482**, 49 (2008).

²⁶Z. Zhang, Y. Wang, D. Wang, Y. Zhou, K. Otsuka, and X. Ren, *Phys. Rev. B* **81**, 224102 (2010).

²⁷P. Lloveras, T. Castán, M. Porta, A. Planes, and A. Saxena, *Phys. Rev. B* **81**, 214105 (2010).